Analog modulation by flexoelectric effect in liquid crystals

W. C. Yip[1], Chris Welch[2], Georg H. Mehl[2] and Timothy D. Wilkinson[1]

[1]*Department of Engineering, University of Cambridge, 9 JJ Thomson Avenue, Cambridge, CB3 0FA, UK.*
[2]*Department of Chemistry, University of Hull, Hull, HU6 7RX, UK.*
Corresponding author: larry.wc.yip@ieee.org

We have solved the long-standing problems of stability and hysteresis, and we are able to obtain the homogeneous uniform lying helix structure in polymer-free cholesteric liquid crystals. This is instrumental for the present work to demonstrate the analog modulation at high speed and high precision. The device is configured for the transverse field switching wherein the substrate surface is flat. In addition to the response time of 10 micro-seconds at room temperature, we have obtained the R-squared and the adjusted R-squared as a measure of true sine-wave for the sinusoidal responding transmission from 1 Hz to 100 kHz that are all greater than 0.9993. In Michelson interferometer, the phase shift at wavelength 633 nm after two passes has been measured equal to about π/9 at 4.6 V/μm for the chiral-doped nematic mixtures E7.

1. Introduction

Liquid crystal modulator that can operate in analog mode at high speed and high precision is always a broad interest particularly for the spectroscopic polarimetry applications. Because the resonance frequency shift and vibration intensity instability in association with the photo-elastic modulator are still problems to be solved. One of the high speed liquid crystal devices was first invented by James L. Fergason in 1984 (US Patent No: 4,436,376). It was based on nematic liquid crystal mixtures to modulate and demodulate the light beam in a communication system. There was a signal linearity problem that made the proposal impractical. It had been found that the demodulated light beam had the same frequency as the input sawtooth wave but it exhibited many sub-harmonic components of the input sawtooth wave. To mitigate this problem, one of the challenges was to fabricate two identical liquid crystal devices to produce a signal of the type wherein the sawtooth linearity of the output signal became apparent. In 1987, Doane *et al* developed so called a polymer dispersed liquid crystal (PDLC) device [1]. The response time to the electric field was less than 0.3 milli-seconds whereas the time required for the film to relax back to the scattering state was about 3 milli-seconds. In an independent study by Basile *et al*, the total phase shift induced by PDLC was reported difficult to control [2]. It depends on the polarization and propagation direction of incident light, the liquid crystal orientation inside the droplet and the droplet orientation with respect to the electric field. These limit the use of PDLC devices. Early research in ferroelectric liquid crystal materials was found in the work of Heilmeier and his co-worker in 1966 [3] and in an often cited paper by Meyer in 1975 [4]. In 1980, Clark *et al* disclosed a liquid crystal device that allowed the molecular directors to rotate between two stable orientations in the micro-second regime [5]. In this device, the substrates are put sufficiently close together so that the intrinsic helical configuration which is present in the bulk will be suppressed. It is referred to as the surface stabilized ferroelectric liquid crystal (SSFLC) device. The switching is very fast but it is restricted to the bistable operation. In 1994, Sharp *et al* reported the analog modulation in 25 μs response time by the electroclinic effect [6]. Smectic liquid crystal materials were used and the device was operated near the C* to A* transition. The phase shift limited by the electroclinic effect was less than 35 degree in a single pass. Large tilt angle exceeding 45 degree and high transmission in red green and blue of the visible spectrum were obtained by Fünfschilling *et al* in 1996 although two deformed helix ferroelectric devices were required for the optimal performance [7]. There is however a change in the birefringence of liquid crystal material intrinsic to the deformed helix ferroelectric effect [8]. This has been reported problematic for the control of polarization state. In 2009, Castles *et al* worked on the transmission effects of flexoelectro-optic director deformation in a Grandjean texture (also known as the uniform standing helix structure) [9]. The authors showed that this effect enabled fast switching in about 17 μs response time and it had low chromatic dispersion over the visible spectrum. By using Berreman method, it was further predicted that the contrast ratio at normal incidence was 1500 to 1 at a switch-on tilt angle of 41.5 degree when an in-plane electric field 19.8 V/μm was applied. The major problem was the requirement of special IC driver that can provide high operation voltage with a sufficient bandwidth.

In 1990, Meyer *et al* discussed in their patent (US Patent No: 4,917,475) that the only proposal of the flexoelectric effect in cholesteric liquid crystal materials was first found in Durand *et al* in 1986. Since early 2000, liquid crystal dimers having large flexoelectric coefficients for the full wave modulation have also been synthesized although most of them have high melting point [10]. Nevertheless, it

has been known for many years that the uniform lying helix (ULH) structure critical for the flexoelectric effect is not stable and it will slowly relax back to the Grandjean texture after the removal of electric field. There have been publications and inventions to stabilize the ULH structure but the trade-offs in response time, stability and error caused by hysteresis hammer the exploitation for any practical application. Recently, we have shown how to obtain a ULH structure having stable and reversible characteristics that solves these long-standing problems [11, 12]. In this paper, it is further developed for the analog modulation and it is referred to as the flexoelectric liquid crystal (FlexoLC) modulator shown in Fig. 1.

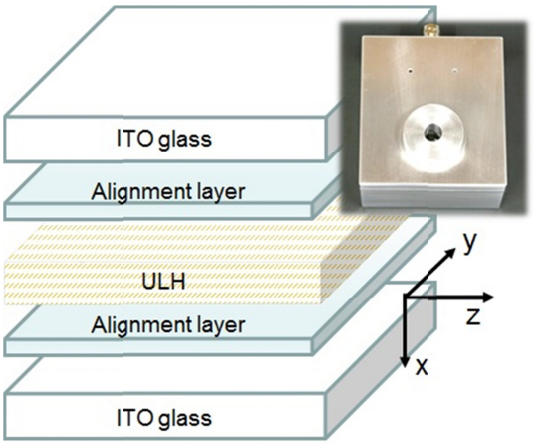

Fig. 1 The device structure and photo of FlexoLC modulator.

2. Theory

In 1969, Meyer extended the idea of Sir Frederick Charles Frank's papers and discovered the so called flexoelectric effect such that the presence of splay-bend deformation in liquid crystals can induce an electrical polarization [13]. Because the deformation will polarize the liquid crystal molecules by acting on the shape polarity and an electric field will distort the structure by aligning the permanent dipole moments. It has been suggested that this effect can be observed readily if the liquid crystal molecules possess a large shape polarity and a large permanent dipole moment parallel to their long dimension. In general, this effect has also been predicted non-zero for the highly symmetric liquid crystal molecules. It is due to the quadrupolar term that will interact with the curvature field to produce a spatial gradient of the quadrupole density and hence the dipole density [14]. So, the free energy density due to the flexoelectric effect is given by

$$f = -e_s E \cdot (\hat{n}\nabla \cdot \hat{n}) - e_b E \cdot (\hat{n} \times \nabla \times \hat{n}) \qquad (1)$$

The splay and bend flexoelectric coefficients are phenomenological and denoted by e_s and e_b respectively. The director field of liquid crystal molecule is modelled by $\hat{n}$ and the electric field is represented by E. This effect has been observed in the nematic, cholesteric and smectic phases particularly in the wedge shape or bend core liquid crystal molecules.

For the flexoelectric effect in cholesteric liquid crystals, we recall the equations derived by Patel *et al* [15, 16] and use the same notations. In the following discussion, the ULH structure is formed in cholesteric liquid crystal wherein the helix axis is lying parallel to the substrate surface. In the presence of electric field, the helix axis of ULH structure is rotated by a tilt angle $\emptyset$ about the x-axis. It is assumed that the helix axis of ULH structure is initially along the z-direction. The spatial-homogenous electric field E is applied in the x-direction while the director of cholesteric liquid crystal is parallel to the x-y plane. The equilibrium helical distortion is determined by the balance between the elastic energy and the field energy due to the flexoelectric coupling with the electric field under the assumption of negligible dielectric contribution. Therefore, taking the one elastic constant approximation and for the small rotation, the tilt angle is given by

$$tan(\emptyset) = \bar{e}E/t_0K_1 \qquad (2)$$

where K_1 is the splay elastic constant, t_0 is the equilibrium twist of cholesteric liquid crystal and $\bar{e}$ is the mean flexoelectric coefficient assuming that $\bar{e}=e_s=e_b$. The equilibrium twist is defined as $2\pi/p_0$ where p_0 is the corresponding pitch of cholesteric liquid crystal at equilibrium. Surprisingly, it has been shown by Patel and Meyer that Eq. (2) still holds when the dielectric anisotropy is not negligible [15]. In addition, according to the balance of torque equation that governs the dynamics of helix rotation, the characteristic time for small rotation is given by

$$\tau = \gamma_1/t_0^2K_1 \qquad (3)$$

where γ_1 is the viscosity of pure rotation. It is determined by the material constants and the equilibrium twist, and it is independent of the electric field. When the elastic constants are not equal, Rudquist *et al* [17] have obtained the following equation for the tilt angle in small rotation approximation.

$$tan(\emptyset) = \bar{e}E/t_0K_2 - [(K_1 + K_3)/2K_2 - 1]sin(\emptyset) \qquad (4)$$

where K_2 and K_3 are the twist and bend elastic constants respectively. Since the tilt angle is usually small, Eq. (4) can be reduced to Eq. (2) when K_1 is substituted by the average of K_1 and K_3. In the first order approximation, the authors have also replaced the splay elastic constant in Eq. (3) by the average of K_1 and K_3 to calculate the response time. So, we shall use the average of K_1 and K_3 to

substitute K_1 accordingly. In a cross-polarizers setup, the transmitted intensity and its relative change in term of the incident intensity I_0 are respectively given by

$$I = I_0 sin^2(2\beta) sin^2(\pi \Delta nd/\lambda_0) \quad (5a)$$

$$\Delta I/2I = sin(4\emptyset)/tan(2\beta) \quad (5b)$$

where β is the angle of optic axis relative to the polarizer axis in the absence of electric field. The effective birefringence, thickness of liquid crystal layer and centre wavelength of incident light are denoted by Δn, d and λ_0 respectively. At β=22.5 degree, the relative change in transmitted intensity obtained by Eq. (2) and Eq. (5b) becomes approximately 4 times the electric field. Because the tangent angle becomes comparable to the sine angle in small rotation approximation. To measure the phase shift, the Michelson interferometer setup is used and the beam splitter shown in Fig. 4 (a) divides the light beam into two halves in which the light beam in the sample arm passes the FlexoLC modulator twice. So, the intensity at the detection plane where two light beams interfere is given by

$$I = I_1 + I_2 + 2\sqrt{I_1 I_2} cos(\delta) \quad (6a)$$

where I_1 and I_2 are the intensity of light beam in the reference and sample arms respectively. The intensity of interference fringe is represented by the square root of I_1 and I_2 and it is often referred to as half of the visibility. The phase difference between the light beams in the reference and sample arms is denoted by δ. In view of Eq. (2) under the small rotation approximation, the Jones matrix for the FlexoLC modulator can be reduced to a rotation of optic axis when the half-wave condition is met. This compares with the smectic liquid crystal modulator [18]. Therefore, the rotation of optic axis as a result of change in tilt angle that gives rise to the phase shift is given by the following expression.

$$cos(\delta) = cos^2(\pi \Delta nd/\lambda_0) - sin^2(\pi \Delta nd/\lambda_0) cos(4\emptyset) \quad (6b)$$

This equation holds for the incident light of linear or circular polarization. The plane of incidence representing the x-axis and the right-hand rule are assumed. Incidentally, this notation is sometimes different from that used by the liquid crystal researchers. For the unified derivation and the reciprocal treatment, the book authored by Chipman *et al* [19] is suggested.

3. Experiments

The FlexoLC modulator comprising the pixel electrodes in transverse field switching configuration was fabricated using the indium tin oxide (ITO) film. Then the metal electrodes that were in contact with the pixels were fabricated using the chromium film. Negative photoresist AZ nLOF 2020 from MicroChemicals was spin-coated at 4000 rpm for 30 seconds before it was baked at 100 ^{0}C for 1 min. It was then exposed to UV light and it was post baked at 110 ^{0}C for 1 min before it was developed in AZ 726 MIF for 90 seconds. The layer of chromium was deposited by sputtering. Lift-off in 1-Methyl-2-pyrrolidon (NMP) and resist stripping by oxygen plasma were followed. Azo-dye film was spin-coated on top of the electrode and it was baked at 80 ^{0}C for 15 min. The azo-dye material, characterization and device fabrication can be found in the report by Yip *et al* [12, 20]. It was exposed in proximity to a linearly polarized UV light at 5 J/cm^2. A quartz photo-mask was used to transfer the image to the illuminated region. A polymer-free cholesteric liquid crystal mixture comprising E7 and R5011 from Merck was disposed between the first and second substrates. Both substrates were made of glass material in this case and the perimeter was sealed with Norland NOA 68 UV adhesives. In a microscopic view, small domains were observed growing as the liquid crystal was cooling from the isotropic phase in the presence of an electric field. The electric field was homogeneous and substantially normal to the substrate surface. These small domains coalesced and became large domains having a structure of long thin stripes. These large domains further grew to form a ULH structure comprising aligned domains of splay and bend deformation. The ULH structure was aligned in a preferred orientation induced by the alignment layer. The ULH structure comprising these aligned domains were found having stable and reversible characteristics in addition to a good homogeneity. The equipment we used in the measurements were Olympus optical microscope BX 60, Hewlett Packard UV-visible spectroscopy system 8453, Agilent Technologies digital storage oscilloscope DSO 5034A, Thurlby Thandar Instruments synthesized arbitrary waveform generator TG 1230, Linkam hot stage LTS 350 with controller TMS 94, Thorlabs photo-detector PDA 36A, Canon digital camera EOS 550D and a calibrated high-voltage amplifier. It was noted that the measurements and the photo were taken at 22^{0}C unless it was mentioned otherwise.

4. Results and Discussion

The FlexoLC modulator device 1 and device 2 were fabricated for the modulation of amplitude and phase respectively and they were made according to the same

recipe. For the measurements of optical transmission and response time, the cross-polarizers setup in an optical microscope and a coloured glass long-pass filter cutoff at 610 nm were used. The choice was to compare the measurements by the Helium- Neon laser. For the response time measurement, the device was aligned with the optic axis at 22.5 degree relative to the polarizer axis and the rectangular waveform at 1 kHz was applied. The gap that defined the thickness of liquid crystal layer for device 1 and device 2 were estimated to be 4.2 μm and 4.3 μm respectively by analyzing the interference transmission spectrum. Based on the measurements of tilt angle and response time, the pitch of device 1 was deduced to be about 137 nm which was difficult to be measured accurately by the spectral transmission method. The response time of device 1 was measured as 20 μs, 11 μs and 7 μs at 10 °C, 20 °C and 30 °C respectively [12]. It was equal to 10 μs at room temperature. For device 2, the equilibrium pitch was measured by the spectral transmission method and it was equal to 516 nm. The response time of device 2 was measured equal to 140 μs at room temperature. Although it became slower in response time, it had a larger phase shift as a result of longer pitch. The rise time and fall time were approximately equal and the response time was defined as an average of rise time and fall time. In any of these cases, the response time was found independent of the electric field that was predicted by Eq. (3). In addition, the measurements of response time on the electric field cycling were found showing a temperature-dependent constant value and there was no noticeable hysteresis.

Table 1 Summary of statistical parameters that compare the output sinusoidal responding transmission with the reference model. Notes: (1) No of points, (2) Degrees of Freedom, (3) Reduced Chi-Sqr, (4) Residual Sum of Sqr, (5) R-Squared, (6) Adj. R-Squared and (7) Fit Status.

	1Hz	10Hz	100Hz	1kHz	10kHz	100kHz
1	1000	1000	1000	1000	1000	1000
2	996	996	996	996	996	996
3	0.02749	0.0063	0.00372	0.00206	0.0027	0.00083
4	27.3788	6.27111	3.70641	2.05391	2.69271	0.83021
5	0.99933	0.99991	0.99995	0.99997	0.99996	0.9998
6	0.99932	0.99991	0.99995	0.99997	0.99996	0.9998
7	100	100	100	100	100	100

For the optical transmission measurement, the device 1 was aligned with the optic axis at 22.5 degree relative to the polarizer axis and the sinusoidal waveform at 18 Vpp from 1 Hz to 100 kHz was applied. The statistical parameters that quantified the goodness of fit with reference to the model Waveform of the software Origin were summarized in Table 1. The R-squared and the adjusted R-squared for the sinusoidal responding transmission driven at 1 Hz, 10 Hz, 100 Hz, 1 kHz, 10 kHz and 100 kHz were obtained all greater than 0.9993. The R-squared is equal to 1 when the data are perfectly predicted by the reference model whereas the adjusted R-squared provides an unbiased estimate and it corrects for any overestimation.

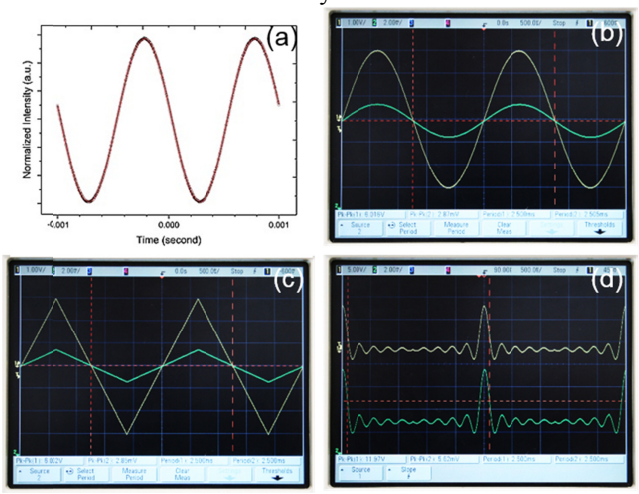

Fig. 2. (a) Plot of sinusoidal transmission fitted by the reference model. Comparisons of (b) sinusoidal transmission, (c) triangular transmission and (d) sinc-function transmission.

In Fig. 2 (a), the sinusoidal responding transmission (black square) was fitted by the reference model (red line). The peak-to-peak voltage and the frequency were 6 Vpp and 1 kHz respectively. In general, the estimated values of parameters are used, in conjunction with the optimization algorithm, to attempt to find the global minimum of a sum of squares. In this case, the convergence was fast and it reached the global minimum after some iterations. In Fig. 3, there was no systematic deviation or biased randomness in the corresponding residual plots. The histogram showed a symmetry approaching the normal shape distribution and the data in the percentile against residual plot was also well behaved in the logarithm scale. So, it was concluded that the true sine-wave response can be obtained for the modulation frequency from 1 Hz to 100 kHz. In addition, the snapshots of sinusoidal responding transmission and triangular responding transmission were captured in Fig. 2 (b) and Fig. 2 (c) respectively. In both cases, the output waveforms in channel 2 (green) were showing a clean and low noise response that faithfully reproduced the waveform of input reference signal in channel 1 (yellow). The peak-to-peak voltage and the frequency of input reference signal were 6 Vpp and 400 Hz respectively in these cases. Since the output signal was measured by the photo-detector, there would be a dc offset in the output waveform. Yet, it was clear that the output waveform followed the change of sign when the polarity of input reference signal was reversed. Furthermore, the transmission on a sinc function input signal at 12 Vpp and 400 Hz was shown in Fig. 2 (d). The output waveform in channel 2 (green) showed a symmetric variation with the extrema that matched the input reference

signal in channel 1 (yellow). The waveform was smooth and had a repeated cycle at the period of 2.5 ms whereas the zero-crossings were following the input reference signal in good synchronization.

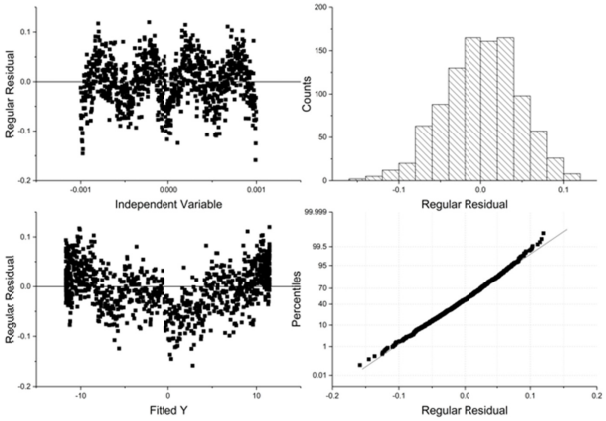

Fig. 3. Plots of residual analysis for Fig. 2 (a) using the software Origin.

To measure the phase shift caused by the FlexoLC modulator, device 2 and the interferometry configuration in Fig. 4 (a) were used. The snapshot of experimental setup was shown in Fig. 4 (b). It comprised Helium-Neon laser (GL), photo-detector (PD), circular polarizer (CP), non-polarizing beam splitter (BS), metallic mirrors (M), prism (P), optical lens (L), diaphragms (D), quarter-wave plates (QWP) and rotation stage to hold the sample (S). The light beam was right-hand circularly polarized at 633 nm and the quarter-wave plate was placed in front of the mirror to retro-reflect the light beam. A pinhole was mounted in front of photo-detector to keep track with the shift in the interference fringe. For the calibration, a snapshot of interference fringe with clear visibility was shown as an insert in Fig. 4 (b) when the FlexoLC modulator was removed from the sample arm. In Fig. 4 (c) and (d), the interference fringes at 0 V and 40 Vpp were shown respectively. The input sinusoidal waveform at 200 Hz was used. The shift in the interference fringe was noticeable although it was small. The central spot size was reduced as the phase was changed from 0 V to 40 Vpp. In Fig. 4 (e), the change in intensity due to the phase shift was captured and the flip of peaks was observed. The corresponding waveform was shown in channel 2 (green) whereas the input sinusoidal waveform at 40 Vpp and 200 Hz was time triggered in channel 1 (yellow). The raw data was acquired electronically and compared with the theory in Fig. 5 (a). The measurement and theoretical prediction by Eq. (6) were represented by black dot and blue line respectively.

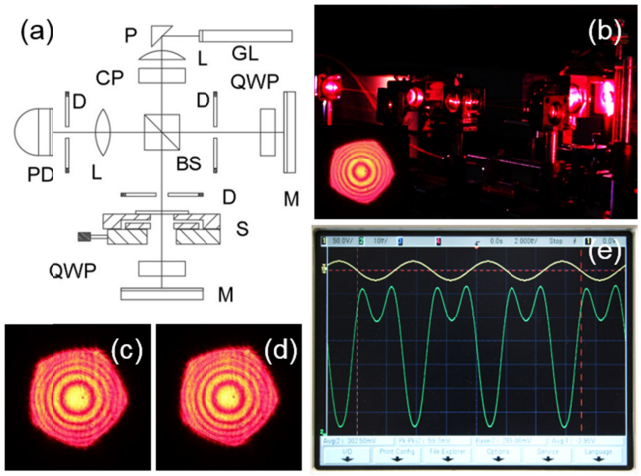

Fig. 4. (a) Configuration and (b) snapshot of interferometry setup for the measurement of phase shift; comparison of interference fringes driven at (c) 0 V and (d) 40 Vpp, and (e) snapshot of change in intensity due to the phase shift at 40 Vpp.

The agreement with the prediction was good and the estimated tilt angle was 5.1 degree at 40 Vpp. So, the phase shift in 2-pass was equal to about $\pi/9$ at 4.6 V/μm. Based on a series of measurements and comparisons, the average transmittance and tilt angle were obtained as a function of electric field. These were plotted for the input sinusoidal waveform at 200 Hz in Fig. 5 (b). The average transmittance, tilt angle and theoretical prediction by Eq. (5) were represented by solid dot, hollow triangle and solid line respectively. In small rotation approximation, the linearly dependence of tilt angle on the electric field was good. When the electric field was increased, a deviation from the linearity became apparent. This trend that was saturated in high electric field had been reported by Rudquist *et al* [21]. The linear response was strongly distorted and dips in the transmitted light intensity were observed. It was due to the decrease in the birefringence caused by the field-induced unwinding of the helix. Likewise, the cause in the present case was attributed to the dielectric coupling that began unwinding the helical pitch when the electric field was sufficiently high. According to our recent results, the unwinding induced an offset in the phase shift which was effectively giving rise to a non-symmetrical rotation about the optic axis at high electric field. As a result, the flip of peaks was observed to be one-sided when the optic axis was aligned initially at 22.5 degree or -22.5 degree relative to the polarizer axis. No such flip of peaks and drift from the average were found at low electric field. We had verified that it was not due to the misalignment of optic axis in the absence of electric field.

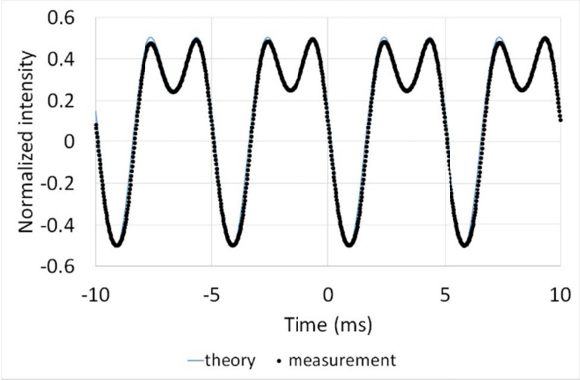

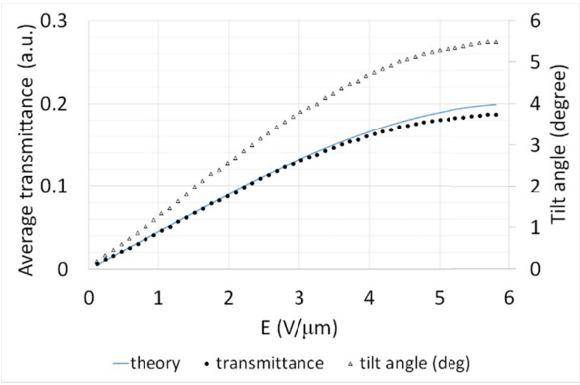

Fig. 5. (a) Plot of normalized intensity for the phase shift at 40 Vpp in 2-pass and (b) plot of average transmittance and tilt angle in 1-pass

5. Conclusions

To summarize, we have developed the FlexoLC modulator that can operate in analog mode at high speed and high precision. The chiral-doped nematic mixture E7 and the transverse field switching electrode configuration are used for the demonstration. In addition to the response time of 10 micro-seconds at room temperature, we have obtained the R-squared and the adjusted R-squared as a measure of true sine-wave for the sinusoidal responding transmission driven at 1 Hz, 10 Hz, 100 Hz, 1 kHz, 10 kHz and 100 kHz that are all greater than 0.9993. We also show that the phase shift as a function of tilt angle can be obtained by the FlexoLC modulator. In small rotation approximation, the phase shift has a linear dependence on the tilt angle and the phase shift at wavelength 633 nm after two passes has been measured equal to about $\pi/9$ at 4.6 V/μm. These results are in good agreement with Meyer's theory on the flexoelectric effect in liquid crystals.

Funding. The EPSRC project number was EP/M016218/1. The project was funded by the Engineering and Physical Sciences Research Council in UK and the project number was EP/M016218/1.

Acknowledgments. This work was based on the PCT application filed in 2017 by Yip *et al* [11] and the device comprising stable ULH structure was further developed for the analog modulation of amplitude, phase and polarization control.

Disclosures. The authors declare no conflicts of interest.

References

1. J. W. Doane, N. A. Vaz, B. G. Wu and S. Žumer, "Field controlled light scattering from nematic microdroplets", Appl. Phys. Lett. **48**, 269-271 (1986).
2. F. Basile, F. Bloisi, L. Vicari and F. Simoni, "Optical phase shift of polymer-dispersed liquid crystals", Phys. Rev. E **48**, 432-438 (1993).
3. R. Williams and G. H. Heilmeier, "Possible ferroelectric effects in liquid crystals and related liquids", J. Chem. Phys. **44**, 638-642. (1966).
4. R. B. Meyer, L. Liebert, L. Strzelecki and P. Keller, "Ferroelectric liquid crystals", J. de Physique Lett. **36**, 69-71 (1975).
5. Noel A. Clark and Sven T. Lagerwall, "Submicrosecond bistable electro-optic switching in liquid crystals", Appl. Phys. Lett. **36**, 899-901 (1980).
6. Gary D. Sharp and Kristina M. Johnson, "High-speed analog complex-amplitude liquid-crystal light modulator", Opt. Lett. **19**, 1228-1230 (1994).
7. Jürg Fünfschilling and Martin Schadt, "Performance of conventional and novel deformed helix ferroelectric liquid crystal display operating modes", Jpn. J. Appl. Phys. **35**, 5765-5774 (1996).
8. L. A. Beresnev, V. G. Chigrinov, D. I. Dergachev, E. P. Poshidaev, J. Fünfschilling and M. Schadt, "Deformed helix ferroelectric liquid crystal display: A new electrooptic mode in ferroelectric chiral smectic C liquid crystals", Liq. Cryst. **5**, 1171-1177 (1989).
9. F. Castles, S. M. Morris and H. J. Coles, "Flexoelectro-optic properties of chiral nematic liquid crystals in the uniform standing helix configuration", Phys. Rev. E **80**, 031709 (2009).
10. Corrie T. Imrie and Peter A. Henderson, "Liquid crystal dimers and higher oligomers: between monomers and polymers", Chem. Soc. Rev. **36**, 2096–2124 (2007).
11. W. C. Yip and Timothy D. Wilkinson, Liquid crystal devices and method for manufacturing liquid crystal devices, World Intellectual Property Organization, WO2018192862 (2018).
12. W. C. Yip, Chris Welch, Georg H. Mehl and Timothy D. Wilkinson, "A cholesteric liquid crystal device having stable uniform lying helix structure", to appear in J. Mol. Liq.
13. Robert B. Meyer, "Piezoelectric effects in liquid crystals", Phys. Rev. Lett. **22**, 918-921 (1969).
14. Robert B. Meyer, "Introduction to flexoelectricity: Its discovery and basic concepts" in *Flexoelectricity in liquid crystals: Theory, experiments and applications* (Imperial College Press, 2013), pp. 1-8.
15. J. S. Patel and Robert B. Meyer, "Flexoelectric electro-optics of a cholesteric liquid crystal", Phys. Rev. Lett. **58**, 1538-1540 (1987).
16. J. S. Patel and Sin-Doo Lee, "Fast linear electro-optic effect based on cholesteric liquid crystals", J. Appl. Phys. **66**, 1879-1881 (1989).
17. P. Rudquist, T. Carlsson, L. Komitov and S. T. Lagerwall, "The flexoelectro-optic effect in cholesterics", Liq. Cryst. **22**, 445-449 (1997).
18. Jay E. Stockley, Gary D. Sharp, Dave Doroski and Kristina M. Johnson, "High-speed analog achromatic intensity modulator", Opt. Lett. **19**, 758-760 (1994).
19. Russell A. Chipman, Wai Sze Tiffany Lam and Garam Young, *Polarized light and optical systems* (CRC Press, 2018).
20. W. C. Yip, H. S. Kwok, V. M. Kozenkov and V. G. Chigrinov, "Photo-patterned e-wave polarizer", Displays **22**, 27-32 (2001).
21. P. Rudquist, L. Komitov and S. T. Lagerwall," Linear electro-optic effect in a cholesteric liquid crystal", Phys. Rev. E **50**, 4735-4743 (1994).